Chaotic time-dependent billiards

Alexander Loskutov and Alexei Ryabov
Physics Faculty, Moscow State University, Moscow 119899 Russia

Abstract

A billiard in the form of a stadium with periodically perturbed boundary is considered. Two types of such billiards are studied: stadium with strong chaotic properties and a near-rectangle billiard. Phase portraits of such billiards are investigated. In the phase plane areas corresponding to decrease and increase of the velocity of billiard particles are found. Average velocities of the particle ensemble as functions of the number of collisions are obtained.

Keywords: chaos, billiards, phase portraits

1 Introduction

A notion of billiard in physics is known since G.Bikhoff [1] who considered a problem concerning the free motion of a point particle (billiard ball) in some bounded manifold. So, the billiard dynamical system can be introduced as follows. A billiard table Q is a Riemannian manifold M with a piecewise smooth boundary ∂Q. The billiard particle freely moves in Q. Reaching the boundary, it is reflected from it elastically. Thus, the billiard particle moves along geodesic lines with a constant velocity. In the present article we consider billiards in Euclidean plane. In this case the angle of incidence of the particle is always equal to the angle of reflection.

In accordance with the boundary geometry, dynamics of the billiard particle can be integrable [3], completely chaotic [5, 6] and, depending on the initial conditions, regular or chaotic [4, 7, 8, 10].

A natural physical generalization of the billiard problem is perturbation of the boundary in one or another manner. For the first time, this problem concerning collisions of particles with massive moving scatterers has been considered by S.Ulam [12] in the context of the unbounded increase of energy in periodically forced Hamiltonian systems. It goes back to the question related to the origin of high energy cosmic particles [11] and known as Fermi acceleration. The Fermi–Ulam model has

been the first system where invariant curves, chaotic layers and stable islands have been investigated (details see in [13]). It has been shown that in the case of a quite smooth perturbation of the boundary the particle velocity is bounded by invariant curves. Otherwise, the velocity can grow indefinitely.

For low-dimensional *integrable* billiards the problem of Fermi acceleration has been studied on the example of circle and elliptic billiards [2, 3, 14]. In these papers the authors come to conclusion that the velocity of the particle ensemble is bounded by the corresponding invariant curves. Investigations of *chaotic billiards* have been performed for the Lorentz gas [15, 16]. As predicted, perturbations of the boundary of such a billiard lead to the appearance the Fermi acceleration for the particle. In addition, the acceleration is higher in the case of periodical boundary oscillations than in for their stochastic perturbations.

In the present paper we study so-called stadium-like billiards [10] which are defined as a closed domain Q with the boundary ∂Q consisting of two parallel lines and two focusing curves (Fig.1). If parameter b is a sufficiently small then the billiard is a near-integrable system. In this case its fixed points are stable. As a result, in the stochastic (or chaotic) "sea" the stability regions appear which consist of invariant curves. At the same time, owing to a weak nonlinearity, dynamics near the separatrixes divided the stability regions of elliptic points is chaotic, and the particle can reach neighbourhoods of all points in the chaotic layer. In the case of the fixed boundary the particle dynamics can be both chaotic and regular, depending on the initial conditions. Introduction of external perturbations leads to the possibility of the particle passage from chaotic region to the regular one and back. This is the reason of new interesting effects which are also described in the paper.

2 Definitions and maps

In this section, basic analytical results are presented. They are necessary for the further description of the billiard dynamics.

2.1 Stadium-like billiard with the fixed parabolic focusing components

Consider a billiard shown in Fig.1. To describe its dynamics let us construct the corresponding dynamical system for $b \ll a$. For this, we use the known method of specular reflections. It consists of the reflection of the billiard table form neutral

components. As a result, the stadium is replaced by a caterpillar billiard. It can be shown that the change in the particle velocity in both cases is the same. In addition, one can show that between trajectories of the initial billiard and the obtained "caterpillar", a one-to-one correspondence takes place.

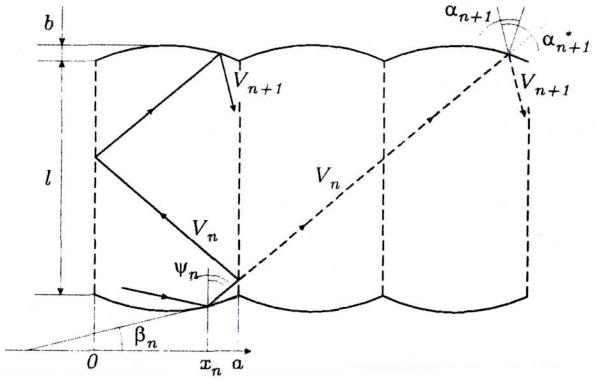

Figure 1: *A stadium-like billiard and its development.*

Suppose that at the initial time the particle belongs to the billiard boundary and its velocity vector directs towards the interior of the billiard region. Let us choose coordinates ψ and x as shown in Fig.1. The motion of the billiard particle induces a map $(\psi_n, x_n) \to (\psi_{n+1}, x_{n+1})$. Suppose that $b \ll l$. In this case the focusing components can be approximated by the function $\chi(x) = 4bx(x-a)/a^2$. For such billiard configuration the map is written as follows:

$$x_{n+1} = x_n + l \tan \psi_{n+1} \ , \ \mathrm{mod}\ a \ ,$$

$$\psi_{n+1} = \psi_n - 2\beta(x_{n+1}) \ ,$$

where $\beta(x) = \arctan(\chi'(x))$ (see Fig.1). If b is small then $\beta \approx 4b(2x-a)/a^2$. For the further analysis change the variables: $\xi = x/a$, $\xi \in [0,1)$. Then

$$\begin{aligned} \xi_{n+1} &= \xi_n + \frac{l}{a} \tan \psi_n \ , \ \mathrm{mod}\ 1 \ , \\ \psi_{n+1} &= \psi_n - \frac{8b}{a}(2\xi_{n+1} - 1) \ . \end{aligned} \tag{1}$$

In Fig.2 the phase portrait generated by the map (1) is shown. Initial conditions for each trajectory are marked by crosses. One can see that the trajectory with initial conditions in the chaotic region can reach any point of this region. At the same time, in the regular regions the points moves along invariant curves.

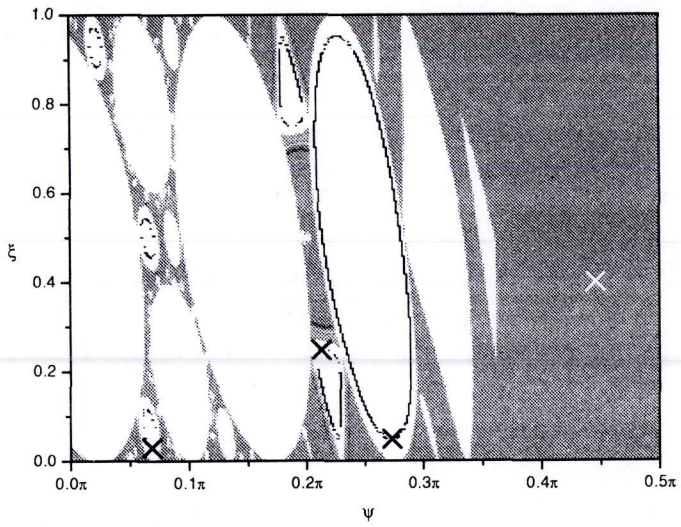

Figure 2: *Phase portrait of the billiard with parabolic focusing components (see map (1)) at $a = 0.5$, $b = 0.01$ and $l = 1$. The diagram contains three regular trajectories (each by 10^7 iterations) and one chaotic trajectory ($5 \cdot 10^8$ iterations).*

It is obvious that the fixed points of the map (1) are the following: $\xi = 1/2$ and $\psi_s = \arctan(ma/l)$. If $m = 0$ then the billiard particle moves strictly vertically. If $m = 1$ then it moves for one cell. And so on. In Fig.2 the fixed points correspond to maximal ellipses. Let us find the stability conditions of these points. To this end, change the variables: $\xi_n = \Delta\xi_n + 1/2$, $\psi_n = \Delta\psi_n + \arctan(ma/l)$ and linearize the map. Then we get:

$$\Delta\xi_{n+1} = \Delta\xi_n + \frac{l}{a\cos^2\psi_s}\Delta\psi_n \ + O(\Delta\psi_n^2) \ ,$$

$$\Delta\psi_{n+1} = \Delta\psi_n - \frac{16b}{a}\Delta\xi_{n+1} \ ,$$

where $\psi_s = \arctan(ma/l)$. The corresponding transformation matrix has the form:

$$A = \begin{pmatrix} 1 & \dfrac{l}{a\cos^2\psi_s} \\ -\dfrac{16b}{a} & 1 - \dfrac{16bl}{a^2\cos^2\psi_s} \end{pmatrix} .$$

It is not hard to see that $\det A = 1$. Thus, the map preserves the phase volume.

The stability criterion for the fixed points is $|\mathrm{TrA}| \leq 2$. Then $\cos^2 \psi_s \geq 4bl/a^2$ or $m^2 \leq l/(4b) - l^2/a^2$. On the other hand, transition to chaos take place if

$$\frac{4bl}{a^2} > 1 \,. \tag{2}$$

Eigenvalues of the matrix A are $\lambda_{1,2} = e^{\pm i\sigma}$, where $\cos\sigma = \frac{1}{2}\mathrm{Tr}A$. Let us introduce $f = l/(a\cos^2\psi_s)$, $g = 16b/a$. In this case

$$A = \begin{pmatrix} 1 & f \\ -g & 1 - fg \end{pmatrix}$$

and its eigenvalues

$$X_{1,2} = \begin{pmatrix} 1 \\ \dfrac{e^{\pm i\sigma} - 1}{f} \end{pmatrix} .$$

Consider matrix X with the columns of eigenvectors. As known, in this case the matrix $\Lambda = X^{-1}AX$ is diagonalization of the matrix A:

$$\Lambda = \begin{pmatrix} e^{i\sigma} & 0 \\ 0 & e^{-i\sigma} \end{pmatrix} .$$

New variables for which the transformation matrix has a diagonal form are the following:

$$\begin{pmatrix} Z \\ Z^* \end{pmatrix} = X^{-1} \begin{pmatrix} \Delta\xi \\ \Delta\psi \end{pmatrix} ,$$

where

$$X^{-1} = \frac{i}{2\sin\sigma} \begin{pmatrix} e^{-i\sigma} - 1 & -f \\ -e^{i\sigma} + 1 & f \end{pmatrix} .$$

One can see that Z and Z^* are complex conjugate. Thus,

$$Z_{n+1} = Z_n e^{i\sigma} \,.$$

If we take Z in the form of $Z = Ie^{i\theta}$ then in the action–angle variables we obtain:

$$\begin{aligned} I_{n+1} &= I_n \,, \\ \theta_{n+1} &= \theta_n + \sigma \,. \end{aligned}$$

Thus, the particle motion around the stable point is written by the map with the following rotation number:

$$\sigma = \arccos\left(1 - \frac{8bl}{a^2\cos^2\psi_s}\right) . \tag{3}$$

In turn, old variables have the form:

$$\Delta\xi = 2I\cos\theta\ ,$$

$$\Delta\psi = \frac{2I}{f}\left(\cos(\sigma+\theta) - \cos\theta\right)\ .$$

Therefore, the Jacobian of the transformation is $J = -\dfrac{4I}{f}\sin\sigma$.

2.2 Perturbations of the boundary and resonance

The particle motion with the velocity V generates a flow for which we can introduce time t. In turn, the time between two sequential collisions is the following: $\tau \approx \dfrac{l}{\cos\psi_s}\dfrac{1}{V}$. Thus, we get the rotation period:

$$T_1 = \frac{2\pi}{\sigma}\tau = \frac{2\pi l}{\cos\psi_s \arccos\Big(1 - 8bl/(a\cos\psi)^2\Big)V}\ .$$

If the system undergoes external perturbations of the boundary of period T_{ext} then for $T_1 = T_{ext}$ we can observe the resonance between degrees of freedom. This leads to the fact that regions including stability areas (see Fig.2) are accessible for the particle.

Some words about the nature of the resonance (see Fig.3). At the motion along the invariant curve in the neighbourhood of the stable point, angle ψ oscillate. Collision of the particle with the perturbed boundary leads to the change in ψ. If the boundary moves towards the particle, then the angle decreases. Otherwise it increases. Suppose that the image of the trajectory moves along the arc AB. In this case, if the particle undergoes collisions coming from the opposite side, then the trajectory tends to inside of the area. If the boundary and the particle velocities have the same direction, then the trajectory goes outside of the region.

For the resonance between the boundary oscillations and the motion along the invariant curve form B to A, collisions change the particle direction. This leads to larger shift of the trajectory to the stable point.

From the equality $T_1 = T_{ext}$ we can obtain the resonance condition for the particle velocity:

$$V_r = \frac{l}{\cos\psi_s \arccos\Big(1 - 8bl/(a\cos\psi_s)^2\Big)}\ . \tag{4}$$

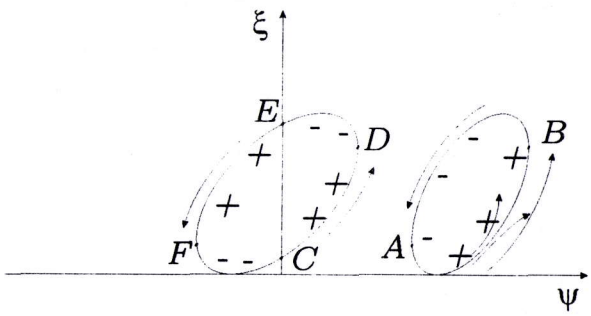

Figure 3: *Invariant curves around stable points (schematically).*

Hereafter, for simplicity we assume that the frequency of external perturbations $\omega = 1$. Then $T_{ext} = 2\pi$.

For the invariant curves with $\psi_s = \arctan(ma/l)$, $m \geq 1$, there exists only one area where the absolute value of the angle ψ_n increases (along the arc AB from A to B in Fig.3), and the area of the decrease in ψ_n. However, for the central stable fixed point there are two such areas: CD, EF for increasing and DE, FC for decreasing. This leads to the fact that in the neighbourhood of this point resonance is observed for the same condition that in the other areas, but the particle velocity is less by half. Therefore,

$$V_r^0 = \frac{V_r}{2} = \frac{l}{\arccos\left(1 - 8bl/a^2\right)} \,. \tag{5}$$

2.3 Focusing components in the form of the circle arcs

In this section, we consider a stadium-like billiard with the boundary consisting of two focusing components in the form of the circle arcs and compare the obtained results with the previous parabolic case.

2.3.1 Fixed boundary

Suppose that focusing components are arcs of the radius R circle (symmetrical about the vertical billiard axis) and the angle measure 2Φ (Fig.4). Geometrically we can obtain that

$$R = \frac{a^2 + 4b^2}{8b} \;;\; \Phi = \arcsin\frac{a}{2R} \,.$$

For such a billiard the chaoticity condition is obtained as follows [9]. Assume that $Q \subset R^2$ and the focusing component is a part of the circle C. Chaos can be observed

if disk D, $\partial D = C$, belongs to the billiard table Q. Thus,

$$\frac{l}{2R} = \frac{4bl}{a^2} > 1 \ ,$$

that is the same as (2) obtained from the analysis of the stable points.

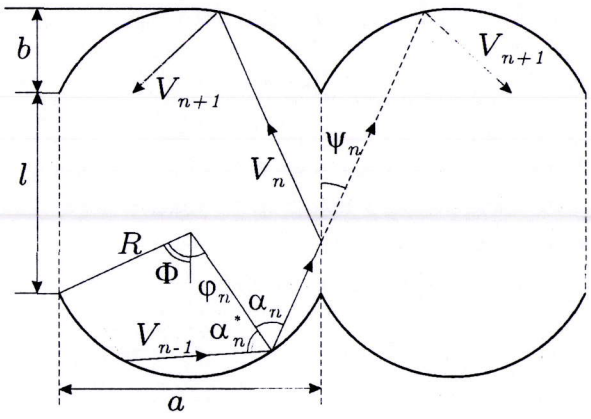

Figure 4: *A stadium-like billiard with focusing components in the form of circle arcs.*

Let us introduce dynamical variables as shown in Fig.4. Assume that angles φ_n and α_n^* are counted counterclockwise, and the angle α_n is counted clockwise. For the fixed boundary $\alpha_n^* = \alpha_n$. Suppose that V_n is the particle velocity, and t_n is a time of n-th collision. Let us find a map describing dynamics of the particle in such a billiard. For this it is necessary to consider two cases: 1) After collision with the focusing component the particle collides with the same component (multiple collisions); 2) After the collision, the particle moves to the opposite focusing component.

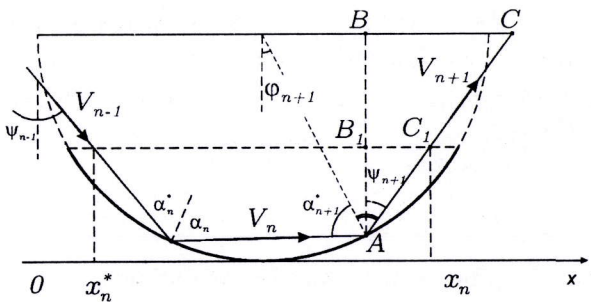

Figure 5: *Multiple collisions with the focusing component.*

1) Multiple collisions (Fig.5).

In this case, geometrically we get the following map:

$$\begin{aligned}
\alpha^*_{n+1} &= \alpha_n \ , \\
\alpha_{n+1} &= \alpha^*_{n+1} \ , \\
\varphi_{n+1} &= \varphi_n + \pi - 2\alpha_n \ (\mathrm{mod}\ 2\pi) \ , \\
t_{n+1} &= t_n + \frac{2R\cos\alpha_n}{V_n} \ .
\end{aligned} \tag{6}$$

If $|\varphi_{n+1}| < \Phi$, then the particle collides with the same component. Otherwise, $n+1$-th collision with the opposite components takes place.

2) Collision with opposite components.

For this case the map can be written as follows:

$$\begin{aligned}
\alpha^*_{n+1} &= \arcsin\left[\sin(\psi_n + \Phi) - \frac{x^*_{n+1}}{R}\cos\psi_n\right] \ , \\
\alpha_{n+1} &= \alpha^*_{n+1} \ , \\
\varphi_{n+1} &= \psi_n - \alpha^*_{n+1} \ , \\
t_{n+1} &= t_n + \frac{R(\cos\varphi_n + \cos\varphi_{n+1} - 2\cos\Phi) + l}{V_n\cos\psi_n} \ ,
\end{aligned} \tag{7}$$

where

$$\begin{aligned}
\psi_n &= \alpha_n - \varphi_n \ , \\
x_n &= \frac{R}{\cos\psi_n}[\sin\alpha_n + \sin(\Phi - \psi_n)] \ , \\
x^*_{n+1} &= x_n + l\tan\psi_n \ (\mathrm{mod}\ a) \ .
\end{aligned}$$

Really, let us extend the circle arc up to the semicircle (Fig.5). Introduce the angle ψ between the vertical and the velocity vector. It is counted clockwise. It is obvious that $BC = R\cos\varphi_{n+1}\tan\psi_{n+1}$. From triangles ABC and AB_1C_1 we get: $\frac{B_1C_1}{BC} = \frac{AB_1}{AB} = \frac{R(\cos\varphi_{n+1} - \cos\Phi)}{R\cos\varphi_{n+1}}$. Therefore,

$$B_1C_1 = R\tan\psi_{n+1}(\cos\varphi_{n+1} - \cos\Phi) \ .$$

Now, using the value x_n for the next collision we obtain:

$$\begin{aligned}
x_{n+1} &= R\sin\Phi + R\sin\varphi_{n+1} + R\tan\psi_{n+1}(\cos\varphi_{n+1} - \cos\Phi) = \\
&= \frac{R}{\cos\psi_n}(\sin\alpha_n + \sin(\Phi - \psi_n)) \ .
\end{aligned} \tag{8}$$

In addition,

$$x^*_{n+1} = x_n + l\tan\psi_n \pmod a \ .$$

If we invert the particle motion then the expression (8) gives connection between x^*_n and α^*_n. This fact allows us to get the explicit system (7).

2.3.2 Perturbed boundary

Suppose that focusing components are perturbed in such a way that their velocity in each point is the same and directed by the normal to the component. Assume that the velocity value depends on time as follows: $U(t) = U_0 f(\omega(t+t_0))$, where ω is a frequency oscillation. We consider the case $U_0/\omega \ll l$, i.e. the shift of the boundary is small enough and can be neglected. Therefore, the billiard map is written as follows:

$$\begin{aligned} V_n &= \sqrt{V_{n-1}^2 + 4V_{n-1}\cos\alpha^*_n U_n + 4U_n^2} \ , \\ \alpha_n &= \arcsin\left(\frac{V_{n-1}}{V_n}\sin\alpha^*_n\right) \ , \end{aligned} \tag{9}$$

$$\left.\begin{aligned} \alpha^*_{n+1} &= \alpha_n \ , \\ \varphi_{n+1} &= \varphi_n + \pi - 2\alpha_n \pmod{2\pi} \ , \\ t_{n+1} &= t_n + \frac{2R\cos\alpha_n}{V_n} \ , \end{aligned}\right\} \quad if\ |\varphi_{n+1}| \le \Phi \tag{10}$$

$$\left.\begin{aligned} \psi_n &= \alpha_n - \varphi_n \ , \\ x_n &= \frac{R}{\cos\psi_n}\left[\sin\alpha_n + \sin(\Phi - \psi_n)\right] \ , \\ x^*_{n+1} &= x_n + l\tan\psi_n \pmod a \ , \\ \alpha^*_{n+1} &= \arcsin\left[\sin(\psi_n + \Phi) - \frac{x^*_{n+1}}{R}\cos\psi_n\right] \ , \\ \varphi_{n+1} &= \psi_n - \alpha^*_{n+1} \ , \\ t_{n+1} &= t_n + \frac{R(\cos\varphi_n + \cos\varphi_{n+1} - 2\cos\Phi) + l}{V_n\cos\psi_n} \ . \end{aligned}\right\} \quad if\ |\varphi_n + \pi - 2\alpha_n| > \Phi \tag{11}$$

The given map describes a stadium-like billiard with the focusing components in the form of the circle arcs. This map is exact one except for the approximation $U_0/\omega \ll l$. The first group (10) corresponds to sequential multiple collisions with one of the focusing components, and the second group (11) corresponds to the passage to the opposite side of the boundary.

3 Numerical analysis

In this Section we consider stadium-like billiards with constant and perturbed boundaries. In the first case, the particle dynamics is described by the exact map (1)

and approximate map (6)–(7), respectively.

3.1 Phase diagrams of billiards with the fixed boundaries

Phase portrait can help to understand the system dynamics and define chaotic and regular regions in its phase space. In Fig.2 the phase diagram of the billiard with the fixed parabolic boundary is shown (see map (1). Crosses in this figure are initial conditions. One can see that phase plane is divided into regular and chaotic regions. If the initial conditions belong to the regular region then the trajectory remains here and forms the corresponding invariant curves. However, beginning in chaotic region the phase trajectory uniformly covers this region. The described portrait has been obtained on the basis of three regular trajectories (each contains 10^7 iterations) and one chaotic trajectory ($5 \cdot 10^8$ iterations) of the map (1). Geometric size of the billiard is the following: $a = 0.5$, $b = 0.01$, $l = 1$.

Figure 6: *Phase portrait of stadium-like billiard with focusing components in the form of circle arcs (see map (6)–(7)). Parameters of the billiard are the same as in Fig.2. One can see nonuniformity of the covering of the chaotic region.*

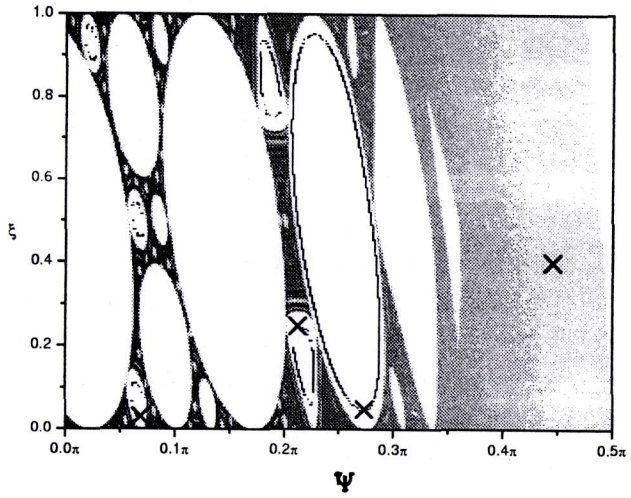

In Fig.6 similar results concerning the map (6)–(7), where the depth of the focusing components is taken into account, are shown. Remind that for this map

the approximation $b \ll l, a$ has been used. To reasonable comparison, the geometric sizes of the billiard and the number of trajectories have been chosen the same as in the previous case (Fig.2).

The difference between obtained diagrams can be easily explain by means of Fig.7.

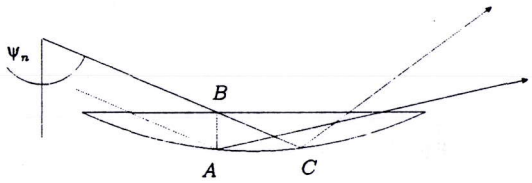

Figure 7: *The difference between the exact billiard map and approximate map.*

Approximation of a small enough depth of the focusing component for the map (1) means the following. Let B be an intersection point of the parabola ends and the particle trajectory. In approximation, we consider the particle collision in the point A which is a projection of B into the arc. But, in fact, the point C is the collision point. As a result, in the exact case for large enough ψ, collisions happen mainly with the right (in the Figure) part of the arc, and from collision to collision the angle ψ decreases. Thus, the billiard particles as if "push out" to the region of the small angel ψ. This is in agreement with Fig.6 where the region $\psi < \pi/2$ is empty..

3.2 Perturbed map

In this section we consider the problem of the velocity change depending on its relation to the resonance value (4).

3.2.1 Phase diagrams

Consider the map (9)–(11) corresponding to the perturbed stadium-like billiards. Construction of the phase diagrams have been performed for the same values of geometric parameters as in the previous §3.1. Therewith, the amplitude of oscillations $U_0 = 0.01$. As noted above (see §2.2), for various particle velocities the corresponding phase portraits should be different form each other.

In Fig.8 the resonance velocity as a function of the angle ψ_s (see (4)) is shown. One can see that in the region form 0 to $\psi_{s\ \max}$ (where $\psi_{s\ \max}$ is a maximal angle for

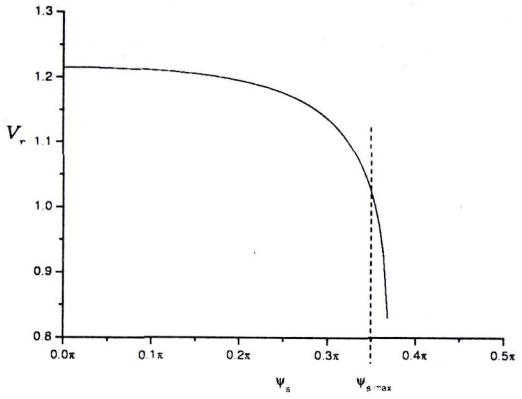

Figure 8: *The resonance velocity as a function of ψ_s (see (4)).*

which the fixed points are still stable) the value of the resonance velocity is varied through a small range.

Phase portraits for the perturbed billiard are shown in Fig.9. For detailed numerical analysis three particle ensembles with initial value $V_0 = 1$, 1.2 and 1.5 have been considered. Therewith initial conditions have been chosen in the chaotic region in a random way. Thus, the obtained portraits give an insight into the velocity change of the billiard particle. In the obtained Figure, the vertical shaded areas correspond to the velocity increasing, and the horizontal shaded areas fit its decreasing. The wait areas (without shading) are the intermediate ones; here the particle velocity is transient. The black tones correspond to the areas which are inaccessible for the phase trajectory.

As follows from obtained diagrams, if $V_0 \neq V_r$ then around the stable fixed points there exist the areas surrounded by invariant curves. As before, these areas are inaccessible for particles from the chaotic regions. At the same time, in the neighbourhood which has become accessible for the particles as a result of perturbations, one can see areas of the increasing and decreasing velocity. Depending on the relation to the resonance velocity value, they can change places.

If $V_0 = V_r$ (the resonance harmonic) then all neighbourhoods of the stable fixed points (except for the central one, $\psi_0 = 0$, $\xi_0 = 1/2$) become accessible for the trajectory. In addition, for this resonance there are no the well-defined areas where the particles have an acceleration.

Following (5) the resonance velocity in the neighbourhood of the central stable

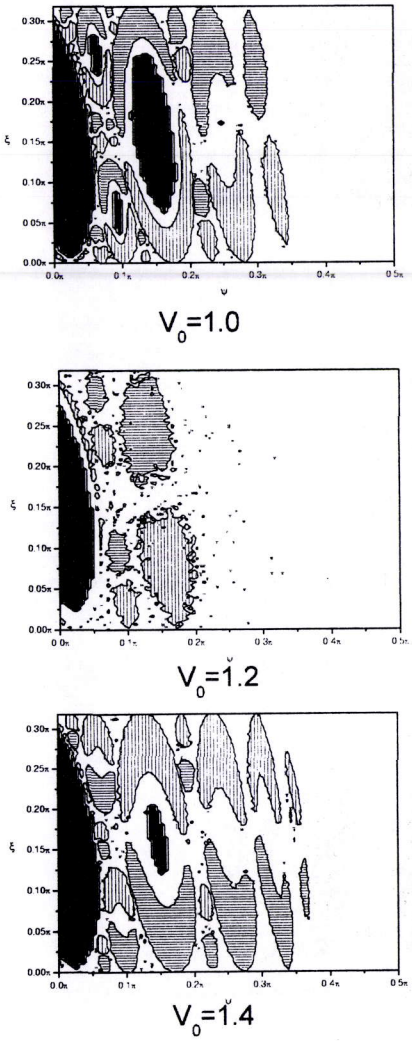

Figure 9: *Phase diagrams of the velocity change in the billiard with the perturbed boundary (see (9)–??eqPertCirBill4)) at* $b = 0.01$, $a = 0.5$, $l = 1$, $U_0 = 0.01$ *and* $\omega = 1$. $V_0 = 1.0$, 1.2 *(resonance)*, 1.5.

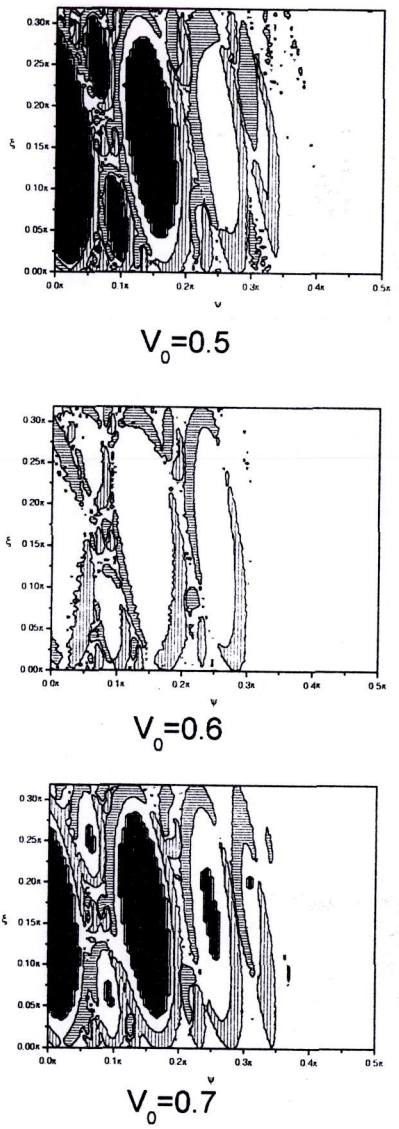

Figure 10: *The same as in Fig.9 but* $V_0 = 0.5$, 0.6 *and* 0.7.

fixed points $V_r^0 \approx 0.6$ (primary resonance). In Fig.10 the phase diagrams for the initial velocities $V_0 = 1$, 1.2 and 1.5 are shown. One can see that at $V_0 = V_r^0$ all areas of the phase space are accessible.

3.2.2 The particle velocity as a function of iterations

Numerical investigations of the perturbed billiard described by the map (9)–(11) have been performed in two cases: when the billiard has strong chaotic properties and for a near-rectangle stadium. In the first case the billiard is a "classical" stadium. Then $\Psi = \pi/2$ and the billiard is a domain with a boundary that consists of two semicircles and two parallel segments tangent to them. The latter case means that focusing components are segments of the almost straight line, and the billiard system is a near-integrable one.

For the first case the following billiard parameters were chosen: $a = 0.5$, $b = 0.25$, $l = 1$, $u_0 = 0.01$, $\omega = 1$, and $V_0 = 0.1$. The particle velocity was calculated as the averaged value of the ensemble of 5000 trajectories with different initial conditions (solid curve 1 in Fig.11). These initial conditions were different from each other by a random choice of the direction of the velocity vector v_0. As follows from the numerical analysis, the obtained dependence has approximately the square-root behaviour ($V(n) \sim \sqrt{n}$). The fitting function $y \sim an^c$ (the dot-and-dash curve 1 in Fig.11) yields the following values: $a = 0.01015 \pm 0.00002$ and $c = 0.4446 \pm 0.0002$.

A near-integrable case means that parameter b (see Fig.4) is a sufficiently small, and the curvature of the focusing components gives rise only weak nonlinearity in the system. In such a configuration the billiard phase space has regions with regular and chaotic dynamics. This case is much more interesting for investigations.

As follows from numerical investigations, on each side of the resonance the behaviour of the particle velocity is essentially different. If the initial value $V_0 < V_c$ then the particle velocity decreases up to a certain quantity $V_{fin} < V_c$, and the particle distribution tends to the stationary one in the interval $(0, V_{fin})$. If, however, $V_0 > V_c$ then billiard particles can reach high velocities. In this case the particle distribution is *not* stationary, and it grows infinitely. In addition, the average particle velocity is also not bounded.

For detailed numerical investigations initial conditions were randomly chosen in the chaotic region of the unperturbed billiard. In Fig.11 the particle velocity as a function of the number of iterations is shown (curves 2–5). The billiard parameters remains the same as for the stadium-like billiard (curve 1) except for $b = 0.01$.

On the basis of 5000 realisations and for every initial velocity, *three curves* have

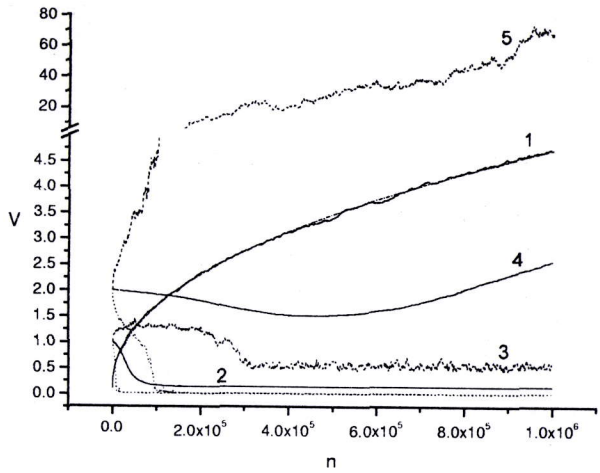

Figure 11: *Average velocity of the ensemble of 5000 particles in a stadium as a function of the number of collisions,* $l = 1$, $a = 0.5$, $U_0 = 0.01$ *and* $\omega = 1$. *Two (dot-dash and solid) curves 1 corresponds to the billiard with strong chaotic properties* ($b = 0.25$). *Curves 2–5 correspond to the near-integrable system* ($b = 0.01$): $V_0 = 1$ *(curve 2, 3) and* $V_0 = 2$ *(curve 4, 5). Curves 2 and 4 are the average velocities of the particle ensemble. Curves 3 and 5 correspond to maximal velocities reached by the particle ensemble to the* n*-th iteration.*

been constructed: the average, minimal and maximal velocities which the particle ensemble has reached to the n-th iteration. So, we can see the interval of the velocity change. As follows from this Figure, if $V_0 < V_c$ then the averaged particle velocity (solid curve 2) gradually decreases and tends to a constant. The maximal velocity of particles (dotted curve 3) also decreases up to V_{fin} and then fluctuate near this value. Eventually, the particle velocities lie in the interval $0 < V < V_{fin}$. In the case of $V > V_c$, the minimal velocity of particles as before decreases. This means that in the ensemble there is a number of particles which are in the region of low velocity values. In our numerical analysis the part of such particles was about 75 percents. At the same time, there are particles with high velocities (dashed curve 5 which corresponds to the maximal velocity of the ensemble). As a result, the averaged particle velocity (solid curve 4) increases.

In Fig.12 a stationary velocity distribution is shown. This distribution was calculated by the one particle trajectory during 10^9 iterations. The initial velocity was chosen as follows: $V_0 \approx V_{fin}/2$. The value denoted by V_{fin} corresponds to the

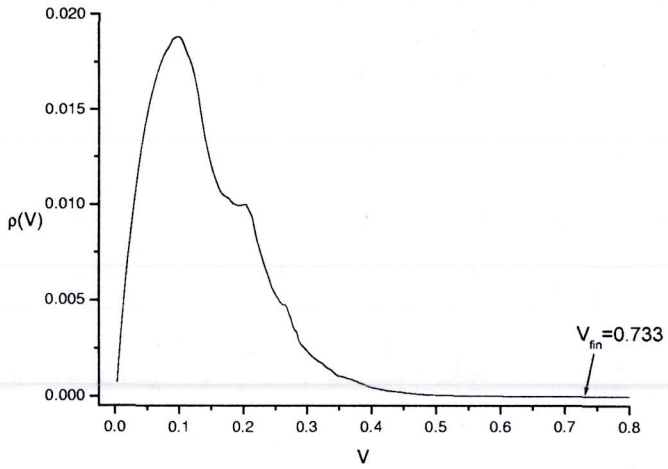

Figure 12: *Stationary distribution of the particle velocity calculated by the one particle trajectory during* 10^9 *iterations.* V_{fin} *is a maximally reached velocity.*

maximally reached velocity.

4 Concluding remarks

Billiards are very convenient models of several physical systems. For example, particle trajectories in billiards of specific configuration can be used in modelling a lot of dynamical systems. Moreover, most approaches to the problems of mixing in many-body systems go back to billiard-like questions. A natural physical generalisation of a billiard system is a billiard whose boundary is not fixed, but varies by a certain law. This is a quite new field which opens new prospects in studies of problems that have been known for a long time.

In the present article we have studied the problem of the billiard ball dynamics in a stadium with the periodically perturbed boundary. Numerical analysis shows that for the case of the developed chaos, the dependence of the particle velocity on the number of collisions has the root character. At the same time, for a near-rectangle stadium an interesting phenomena is observed. Depending on the initial values, the particle ensemble can be accelerated, or its velocity can decrease up to the quite low magnitude. However, if the initial values do not belong to a chaotic layer then for quite high velocities the particle acceleration is not observed.

Analytical description of the considered phenomena (mechanisms of deceleration and acceleration of the billiard particle, stabilisation of unstable points etc.) requires more detailed analysis and will be published soon [17].

References

[1] G.Birkhoff. *Dynamical Systems.*— American Mathematical Society, N.Y., 1927.

[2] J.Koiller, R.Markarian, S.Q.Kamphorst, and S.P.de Carvalho. Time-dependent billiards.— *Nonlinearity* **8**, 983 (1995)

[3] J.Koiller, R.Markarian, S.Q.Kamphorst, and S.P.de Carvalho. Static and time-dependent perturbations of the classical elliptical billiard.— *J. Stat. Phys.* **83**, 127 (1996).

[4] R.Markarian. New ergodic billiards: Exact results.— *Nonlinearity* **6**, 819-841 (1993);

[5] Ya.G.Sinai. Dynamical system with elastic reflection: Ergodic properties of dispersing billiards.— *Russ. Math. Surv.* **25**, 137-188 (1970).

[6] L.A.Bunimovich and Ya.G.Sinai. Statistical properties of Lorentz gas with periodic configuration of scatterers.— *Commun. Math. Phys.* **78**, 479-497 (1981).

[7] L.A.Bunimovich. On ergodic properties of some billiards.— *Func. Anal. Appl.* **8**, 73 (1974)

[8] L.A.Bunimovich. On the ergodic properties of nowhere dispersing billiards.— *Commun. Math. Phys.* **65**, 295-312 (1979)

[9] L.A.Bunimovich. Conditions of stochasticity of two-demensional billiards.— *Chaos* **1**, 187-93 (1991).

[10] G.M.Zaslavsiky. Stochasticity in quantum mechanics.— *Phys.Rep.* **80**, 147-250 (1981)

[11] E.Fermi. On the origin of the cosmic radiation.— *Phys. Rev.* **75**, 1169 (1949).

[12] S.M.Ulam. In: *Proceedings of the 4th Berkeley Symp. on Math. Stat. and Probability.*— University of California Press **3**, 315 (1961).

[13] A.J.Lichtenberg, M.A.Lieberman. *Regular and Stochastic Motion.*— (Springer-Verlag, Berlin, 1983).

[14] M.Levi. Quasiperiodic motions in superquadratic time-periodic potentials.— *Commun. Math. Phys.* **143**, 43-83 (1991).

[15] A.Loskutov, A.B.Ryabov, L.G.Akinshin. Mechanism of Fermi acceleration in dispersing billiards with time-dependent boundaries.— *J. Exp. Theor. Phys.* **86**, 966-973 (1999).

[16] A.Loskutov, A.B.Ryabov and L.G.Akinshin. Properties of some chaotic billiards with time-dependent boundaries.— *J. Phys. A*, **44**, 7973–7986 (2000).

[17] A.Loskutov, A.B.Ryabov.— To be published.